Wide steering angle optical phased array based on silicon nano-membrane

Amir Hosseini, David Kwong and Ray T. Chen

Microelectronic Research Center, Department of Electrical and Computer Engineering, University of Texas, Austin, TX 78758 USA (e-mail: ahoss@ece.utexas.edu; chen@ece.utexas.edu)

ABSTRACT

We present a new approach to wide angle optical beam steering based on nano-membrane-based phased array structures with unequally spaced elements. In our approach, the array elements are positioned in such way that grating lobes associated with different sub-arrays do not overlap. Therefore, we reduce the side-lobe-level of the array radiation pattern and at the same time we can avoid the optical coupling between adjacent waveguides by relaxing the half-wavelength spacing requirement for large angle beam steering. By optimizing the optical waveguide structure for the maximum full-width at half-maximum of the single radiator's radiation pattern we discuss the optimum performance achievable using the Unequally-spaced Waveguide Arrays.

Keywords: Laser beam steering, optical phased array, waveguide arrays, silicon.

1- INTRODUCTION

Fiber Optical phased arrays represent an enabling technology that makes possible simple, affordable, and lightweight laser beam steering with precise stabilization, random access pointing and programmable multiple simultaneous beams. Traditionally, optical beam steering has been achieved through mechanically controlled MEMs system [1] and liquid crystal (LC) based optical phased arrays (OPAs) [2] [3]. Mechanical beam steering provides high steering efficiency and relatively large angle steering. However, the high precision rotating stages are required, which increase the device complexity and are not fast enough for high speed applications. LC OPAs provide rapid random access steering without the expensive and complex mechanical systems [4]. However, LC OPAs suffer from low steering speed (typically milliseconds response time) and limited steering angle (typically not more than 10°) [3]. A GHz optical beam steering system employing phased array waveguides was recently demonstrated with a maximum steering angle of about 6° [5]. The important issue with phased equally spaced array waveguides is the strong coupling between the adjacent waveguides when the waveguide spacing is reduced to about half the wavelength, which is necessary for wide angle beam steering. Therefore, the optical coupling jeopardizes the side lobe level and steering efficiency by imposing a lower limit on the waveguide spacing. Other techniques such as beam steering with electro-wetting micro-prisms [6] and polymeric slab waveguide based thermally-induced beam steering [7] have response time in the order of tens of milliseconds.

So far, the large angle beam steering systems have been based on multi-stage systems combining LC OPAs with holographic glass and birefringent prisms [4], for which, alignment and packaging are very challenging.

In order to suppress the side lobes at large steering angles, an unequally-spaced array structure was proposed [8], [9]. However, an unequally-spaced array realized by random placement [8] of array elements would not result in the optimum OPA performance. An array structure formed by gradually doubling the inter-element spacing across the array can suppress the side lobes [9], but as we show, it severely reduces the steering efficiency. Additionally, the effects of optical radiator structure, finite fabrication accuracy and the achievable performance have not been investigated.

Photonics Packaging, Integration, and Interconnects IX, edited by Alexei L. Glebov, Ray T. Chen,
Proc. of SPIE Vol. 7221, 72210T · © 2009 SPIE · CCC code: 0277-786X/09/$18 · doi: 10.1117/12.809311

In this paper, we report a technique to minimize the side-lobe-level (SLL) in unequally-spaced OPAs while maintaining a steering angle of ±45◦ and avoiding the optical coupling based on sub-arrays with non-overlapping grating lobes. By optimizing both the array structure and the waveguide structure, we present a design methodology for large angle optical beam steering with minimal performance dependence on the steering angle. Finally, we discuss the maximum performance achievable by unequally spaced OPAs and compare it with that of the other non-mechanical beam steering technique based on LC OPAs.

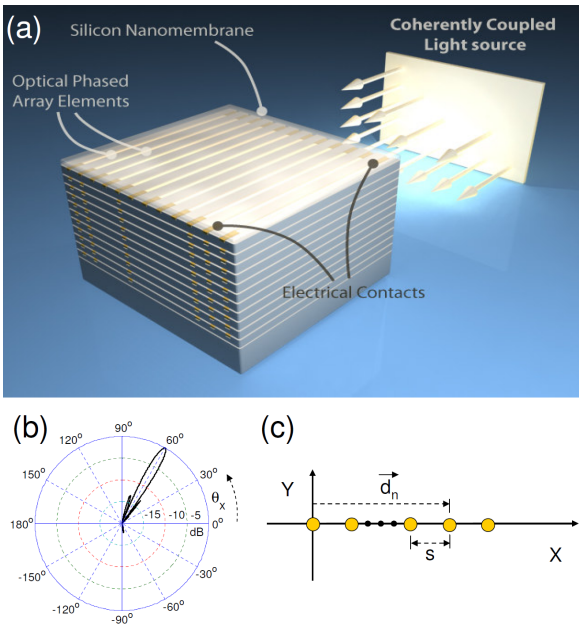

Fig. 1. (a) A schematic of silicon nano-membrane-based OPA beam steering. (b) Far field radiation pattern (array factor only) for 1D uniform array (N=32) with (dn+1-dn) =s=λ/2 and βn+1-βn=156◦. (c) A uniform array structure.

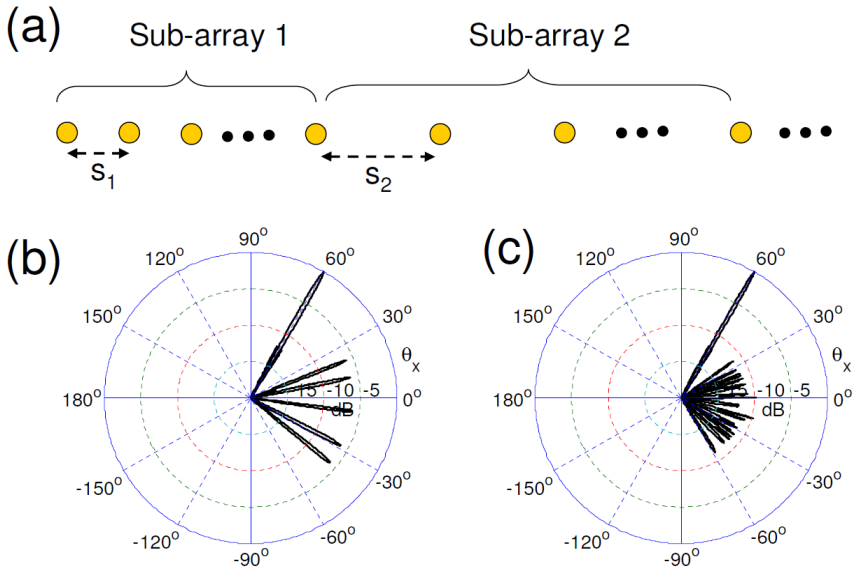

Fig. 2. (a) A schematic of the proposed (1D) unequally spaced OPA structure. Far field radiation pattern for (b) M=2, N=32, q_1=3, q_2=4, s_0=λ/2, (β_2-β_1)/q_1=156˚ and (c) M=4, N=32 q_1=3, q_2=4, q_1=5, q_4=7, s_0=λ/2 and (β_1-β_1)/q_1=156˚.

2- UNEQUALLY-SCPACED ARRAY STRUCTURE

A schematic of a silicon nano-membrane-based OPA system is shown in Figure 1 (a). Similar to their microwave counterparts, linear optical phased arrays consist of 1D or 2D arrays of single-mode waveguides operating at the designated wavelengths. The far-field pattern associated with the array factor is given as $A=\sum_n e^{j\vec{K}.\vec{d}_n+\beta_n}$, where, $\vec{K}$ is the wave-vector ($\left|\vec{K}\right|=\frac{2\pi}{\lambda}$,), and $\vec{d}_n$ is the translational vector of the nth radiator position, β_n is the phase shift of the nth element, and λ is the wavelength (in this paper λ=1.55μm). Beam steering can be done by changing the linear phase shift imposed on each array element. However the maximum steering angle is limited by the appearance of the grating lobes when the spacing between the waveguide-based radiators is more than λ/2. Although a uniform array with half wavelength spacing would allow for grating lobe free beam steering, such spacing between adjacent optical waveguide would result in severe waveguide coupling and therefore, far-field pattern distortion.

In the case of 1D arrays, $\vec{K}.\vec{d}_n=\frac{2\pi\left|\vec{d}_n\right|}{\lambda}\sin\theta_x$, where θ_x (θ_y) is the angle to the Z axis in the XZ (YZ) plane. Considering β_n=0, in a 1D uniform array, where ($|d_{n+1}-d_n|$) =s, for any s>λ, the grating lobes happen at $\theta_{xp}=\sin^{-1}\frac{P\lambda}{s}$, for P=±1, ±2 …, and s>|Pλ|. In the case of $\frac{\beta_n}{d_n}=c$, a constant, the main lobe occurs at $\theta_{x0}=\sin^{-1}\frac{c\lambda}{2\pi}$, independent of s, and the grating lobes are given by $\theta_{xp}=\sin^{-1}\left[\frac{P\lambda}{s}-\sin\theta_{x0}\right]$. Now, consider two 1D uniform arrays with element spacing $s_1=q_1s_0$ and $s_2=q_2s_0$. If $\frac{\beta_n}{d_n}=c$ is the same for the two arrays, then the main lobe occurs the same angle in both cases. Provided that the greatest common divisor (gcd) of q_1 and q_2 is 1, the grating lobes of the two arrays do not overlap, which result in a peak main lobe and equi-ripple side lobes, as shown in Fig. 2(b) and (c).

If s_1 and s_2 are more than one λ, then, the side-lobe-level (SLL), defined as the ratio of the second largest lobe intensity to the maximum intensity (main lobe) [8], is 0dB for each array. However, if the two arrays are placed along each other to form a non-uniform array, the main lobes of each sub-array add up constructively, while the there is no overlap between the peak grating lobes of each sub-array. If these grating lobes are narrow enough, the SLL is reduced to -6dB. Therefore, for narrow enough grating lobes, doubling the number of sub-arrays with non-overlapping grating lobes, can improve the SLL by 6dB. Obviously, the grating lobes corresponding to each sub-array can be arbitrarily narrowed by increasing the number of elements in each sub-array.

Here we formulate the non-uniform array design methodology:

N: the total number of radiators
M: number of sub-arrays
s_i: spacing in group *i,* for *i*=1, 2…
$s_i=q_is_0$
fabrication resolution<s_0<λ/2
gcd(*qi,qj*)=1
s_1>modal size.

Note that s_0 must be smaller than λ/2 in order to avoid overlapping sub-array grating lobes. However, the minimum of s_0 is determined by the fabrication process, or how precisely the waveguides can be placed in the array. In contrast, s_1 does not depend on the fabrication process, but is constrained by the optical coupling between the waveguides; In other words, s_1 must be large enough to avoid waveguide modal field profile overlaps. For the waveguide shown in Fig. 3(a), a center-to-center spacing of 1.5λ~2.4μm (for single mode operating waveguide dimensions W and H < 600nm [see Fig. 3(a)] and λ=1.55μm), diminishes the optical coupling between adjacent waveguides. Note that the presented non-uniform array structure is the first technique to address the optical coupling problem and finite fabrication precision at the same time.

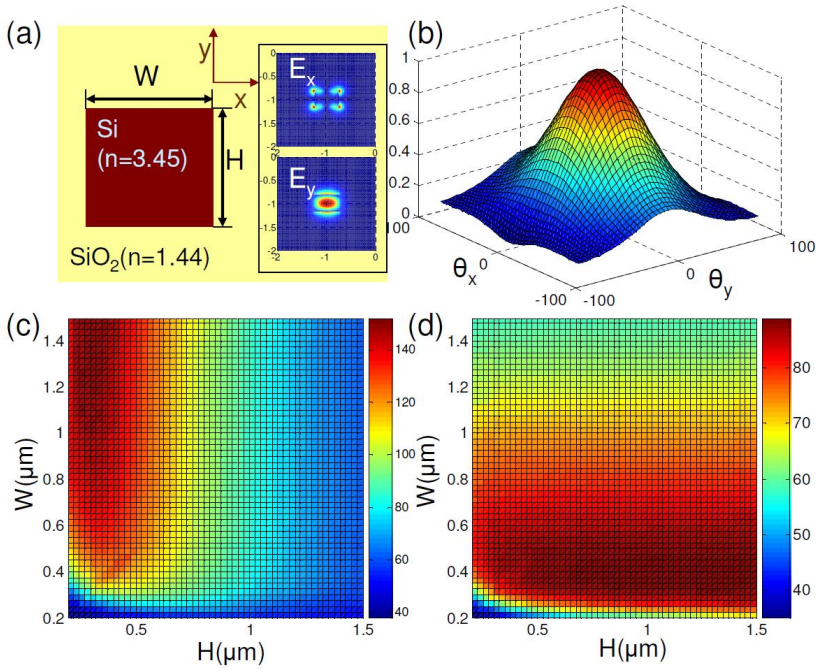

Fig. 3. (a) A schematic of the silicon nano-membrane waveguide; The fundamental TM mode field profiles are shown in the inset. (b) 2D far field radiation of the waveguide shown in (a) assuming W=500nm and H=350nm. (c) and (d). variations of FWHM (in degrees) of En_x and En_y, respectively, with W and H as depicted in (a).

3- OPTIMIZED WAVEGUIDE STRUCTURE

The far field radiation (R) of an OPA is determined by the individual waveguide far field radiation (S), or the envelope, as well as the array factor (A), $R(\theta_x,\theta_y)=A(\theta_x,\theta_y)S(\theta_x,\theta_y)$. A wider envelope allows for larger scanning angles. In order to calculate the envelope, we use Rsoft FEMSIM to generate the waveguide field profiles, and then we calculate the envelope $R=\left|E^2\right|\propto\left|E_\theta^2\right|+\left|E_\phi^2\right|$ using [10]:

$$
\begin{aligned}
E_\theta &= j\frac{e^{-j\frac{2\pi}{\lambda}r}}{r\lambda}\left[\left(f_x\cos\phi+f_y\sin\phi\right)+\eta\cos\theta\left(g_y\cos\phi-g_x\sin\phi\right)\right]\\
E_\phi &= j\frac{e^{-j\frac{2\pi}{\lambda}r}}{r\lambda}\left[\cos\theta\left(f_y\cos\phi-f_x\sin\phi\right)-\eta\left(g_x\cos\phi+g_y\sin\phi\right)\right]\\
\vec{f}(\theta,\varphi) &= \int\vec{E}_t(\vec{r})e^{j\vec{K}.\vec{r}}dr\\
\vec{\mathrm{g}}(\theta,\varphi) &= \int\vec{H}_t(\vec{r})e^{j\vec{K}.\vec{r}}dr
\end{aligned}
\qquad (1)
$$

where, $\vec{E}_t$ and $\vec{H}_t$ are the tangential electric and magnetic field components, and $\eta=120\pi$ is the intrinsic impedance. The integrals are numerically computed over the waveguide cross-sectional plane. Also, note that $\cos\theta=\cos\theta_x\cos\theta_y$ and $\sin\varphi=\sin\theta_x/\sqrt{\sin^2\theta_x+\sin^2\theta_y}$. A schematic of a silicon waveguide is shown in Fig. 3(a). Here we assume the waveguide is excited by the fundamental transverse magnetic (TM) mode input fiber mode. We define the horizontal $[En_h(\theta_x)]$ and vertical $[En_v(\theta_y)]$ envelopes as the variations of the far field radiation pattern [shown in Fig. 3(b)], at $\theta_y=0^\circ$ and $\theta_x=0^\circ$, respectively. Figure 3(c) and (d) depict the full-width-half-maximum (FWHM) of $En_h(\theta_x)$ and $En_v(\theta_y)$, respectively, versus the waveguide width (W) and height (H). As the electromagnetic mode extents out of the waveguide

area for W and $H \le 300nm$, the far field pattern becomes narrow (~40° in both directions). In the case of the TM mode, the field profile extent in the vertical direction is more than that in the horizontal direction. Thus the horizontal envelope is wider than the vertical envelope. As the smaller envelope determines the worst case SLL and the diffraction efficiency, the optimized waveguide dimensions should maximize $En_v(\theta_y)$, while maintaining the single mode condition, $W,H<\lambda/N_{eff}$, where, N_{eff} is the effective index. We find that for W=500nm and H=350nm, the horizontal and vertical FWHM values are 89° and 118°, which allow for about $|\theta_y|\le 45°$ and $|\theta_x|\le 60°$ beam steering in the vertical and horizontal directions, respectively, with maximum 3dB envelope variations. Based on the variations of the envelope in 2D, we expect the worst-case array performance at $\theta_y=\pm 45°$ and $\theta_x=0°$.
Although, here we have assumed the standard silicon fabrication, the performance of presented OPA can be furthere improved using optical waveguide with higher electromagnetic mode confinements (or wider envelopes), such as plasmonic waveguides or High-K core optical waveguides [11].

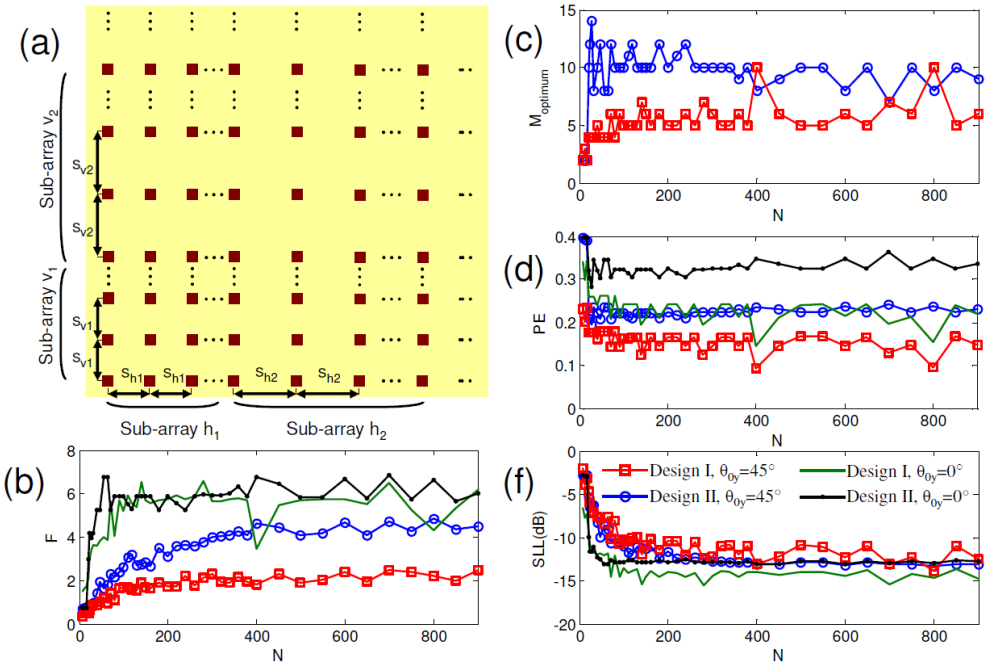

Fig. 4. (a) 2D non-uniform array structure. Variations of the maximum figure of merit (F), the optimum M, power efficiency (PE), and side-lobe-level (SLL) versus N, in (b)-(f), respectively, for Design I (s0=800nm) and Design II (s0=50nm) for the beam steered at $\theta_{0y}=45°$ and $\theta_{0x}=0°$ and also non-steered beam ($\theta_{0y}=0°$ and $\theta_{0x}=0°$). The optimum M for is the same for both steered and non-steered beams in (c).

4- OPTIMIZED ARRAY DESIGN AND PERFORMANCE ANALYSIS

A 2D generalization of the proposed non-uniform array is shown in Fig. 4(a). We consider two parameters to evaluate the performance of the OPA, SLL and the power efficiency (PE), which is defined as the power in the main peak to the power radiated in all angles. For a fixed total number of radiators (N), as the number of groups (M) increases, the SLL decreases, however, since the overlap between the grating lobes of the sub-arrays increases, PE reduces. To find the optimum M to minimize the SLL and maximize the power efficiency, we define a dimensionless figure of merit (F) as

$$F = \frac{PE}{SLL}. \qquad (2)$$

Note that s_0 is a parameter determined by the fabrication process and therefore, we do not take it into account as an independent variable in the optimization process. Now, we consider two designs, Design I: s_0=800nm and Design II: s_0=50nm. In each case, we let N vary, and we find the M value that maximizes F for the worst case scenario (main peak of the steered beam at $\theta_{0y}=45°$ and $\theta_{0x}=0°$). Note that 800nm and 50nm are conservative fabrication resolution assumptions for nano-imprint fabrication techniques and electron beam lithography, respectively [12]. The variations of

F, the optimum M value, PE and SLL with N are shown in Fig. 4. The performance of Designs A and B at a non-steered beam is also depicted.

A smaller s_0 allows for higher PE by reducing the number of grating lobes associated with each sub-array. Therefore, the performance of a non-uniform array with smaller s_0 suffers less from the falling envelope at large angles [Fig. 4(b)]. Furthermore, the optimum M is higher for a smaller s_0 as shown in Fig 4(c). Figure 5(d) shows that the degradation of PE from the non-steered beam to the worst case is only about 30% for both designs. As the SLL of the array factor is independent from the steering angle (θ_0), degradation of the SLL is only determined by the envelope, and in our design it will be about 3dB for large enough N values. At small s_0 values, the side lobes are more concentrated around the main lobe and therefore, degradation of the SLL as the steering angle changes becomes less significant as shown in Figure 4(f). For the non-uniform array structure presented in [8], our calculations show a PE of 0.016, indicating that SLL was decreased at the expense of severe PE degradation.

Based on Figure 4(b), the *F* curves of the non-steered beam saturate at around N=128 and N=64 for Design I and II, respectively. Table I lists the SLL and PE values for these two designs at different steering angles. Note that the steering efficiency, defined as the main peak intensity of the steered beam to the main peak intensity of the non-steered beam [3], is more than 65% in both cases at $\theta_{0x}=0^\circ$ and $\theta_{0y}=45^\circ$. That is because in the case of the unequally spaced array, the dependence of the steering efficiency on the steering angle is merely due to the envelope.

Table. 1. unequally spaced array performance

Design	*F*-curve knee N value	M	Array size (μm)	$\theta_{0x}=0^\circ$ $\theta_{0y}=0^\circ$		$\theta_{0x}=0^\circ$ $\theta_{0y}=45^\circ$		$\theta_{0x}=60^\circ$ $\theta_{0y}=0^\circ$	
				SLL(dB)	PE(%)	SLL(dB)	PE(%)	SLL(dB)	PE(%)
I	128	4	114	-12.1	26.3	-8.5	18.0	-9.0	21.0
II	68	8	300	-13.4	34.6	-9.4	23.4	-10.1	25.7

In conclusion, we present an unequally spaced OPA design for high-efficient large optical beam steering at 1.55 micron, with minimal performance dependence on the steering angle. Assuming fabrication precision of 800nm and 128 array elements, we demonstrate a beam steering with a worst-case power efficiency and side-lobe-level of about 18.0% and -8.5dB during ±60◦ and ±45◦ 2D optical beam steering, which correspond degradation of about 32% and -3.6dB, respectively, with respect to those of the non-steered beam. Increasing the number of array elements and smaller fabrication resolution can improve the performance. The OPA performance dependence on the steering angle is only due to the far-field pattern of single elements, which can be further improved using waveguides that support smaller modal sizes.

REFERENCES

[1] Yves Petremand, Pierre-Andre Clerc, Marc Epitaux, Ralf Hauffe, Wilfried Noell, and N. F. de Rooij, "Optical beam steering using a 2D MEMS scanner", Proc. SPIE, Vol. 6715, 671502, 2007.

[2] Xinghua Wang, Bin Wang, John Pouch, Felix Miranda, James E. Anderson, and Philip J. Bos, "Performance evaluation of a liquid-crystal-on-silicon spatial light modulator ", Opt. Eng., Vol. 43, 2769, 2004.

[3] Xinghua Wang, Bin Wang, Philip J. Bos, Paul F. McManamon, John J. Pouch, Felix A. Miranda, and James E. Anderson, "Modeling and design of an optimized liquid-crystal optical phased array", J. Appl. Phys., Vol. 98, 073101, 2005.

[4] P. F. McManamon, "Agile Nonmechanical Beam Steering," Optics & Photonics News, Vol.17, 24-29, 2006.

[5] Mona Jarrahi, R. Fabian, W. Pease, David A. B. Miller, and Thomas H. Lee, "High-speed optical beam-steering based on phase-arrayed waveguides", J. Vac. Sci. Technol. B, Vol. 26, 2124, 2008.

[6] N. R. Smith, D. C. Abeysinghe, J. W. Haus, and J. Heikenfeld, "Agile wide-angle beam steering with electrowetting microprisms," Opt. Exp., Vol. 14, 6557-6563, 2006.
[7] G. Cocorullo, M. Iodice, "Thermally induced optical beam steering in polymeric slab waveguide". Fibres and Optical Passive Components, Proc. of IEEE/LEOS, 2005.
[8] F. Xiao, W Hu, and A. S. Xu, "Optical phased-array beam steering controlled by wavelength," App. Opt., Vol. 44, 26, pp. 5429–543, 2005.
[9] J. H. Abeles and R. J. Deri, "Suppression of sidelobes in the far-field radiation patterns of optical waveguide arrays," App. Phys. Lett., Vol. 53, No. 15, 1988.
[10] Sophocles J. Orfanidis, "Electromagnetic Waves and antennas", 2004.
[11] J. A. Dionne, L. A. Sweatlock, H. A. Atwater, and A. Polman, "Plasmon slot waveguides: Towards chip-scale propagation with subwavelength-scale localization", Phys. Rev. B, Vol. 73, 035407, 2006.
[12] Helmut Schift, "Nanoimprint lithography: An old story in modern times? A review", J. Vac. Sci. Technol. B Vol. 26, 458, 2008.